Especially, HCV IRES activity was approximately 95%, and most weekly affected by the depletion of PTB. Repletion of PTB to depleted S10 lysate restored activities of PV and EMCV IRESs. The data suggest that PTB plays an important role in picornaviral IRESs, but not in HCV IRES.

Keywords: PTB; HCV; IRES; EMCV; PV; HeLa

Résumé

Dans notre étude, nous avons comparé les effet de la 'polypyrimidine track-binding' (PTB) virus de l'hépatite C (génotype IIa) et l'activité du virus encéphalomyodardite (EMCV) et de l'IRES du poliovirus *in vitro*. La PTB se fixe de manière résistante à l'IRES de l'EMCV mais de manière fragile à l'ARN du PV et du VHC. L'IRES du PV montre la dépendance la plus forte à la PTB et il montre une activité d'IRES de moins de un dixième après immuno-déplétion de la PTB du lysat HeLa10 par des billes d'IgG anti-PTB prêtes à l'emploi, par rapport au HeLa10 traité par des billes d'IgG normales. L'activité de l'IRES de l'EMCV était approximativement égale à 40% de celle sous contrôle normal après déplétion de la PTB. L'activité de l'IRES du VHC était approximativement égale à 95% et la moins sensible à la déplétion de la PTB. La réplétion de la PTB au lysat S10 appauvri rétablit les activités des IRES du PV et de l'EMCV. Les données suggèrent que la PTB joue un rôle important dans les IRES picornaviraux mais pas dans les IRES du VHC. De plus,

Mots clés: PTB; VHC; PTB; IRES; PV; HeLa

1. Introduction

Hepatitis C virus (HCV) possesses a single-stranded RNA (approximately 9610 nucleotides), and classified into the family *Flaviviridae* [1–4]. HCV is a major causative agent of non-A non-B hepatitis, and likely progresses into the chronic hepatitis, cirrhosis and hepatocellular carcinoma.

The 5′ untranslated region (5′UTR) of HCV RNA genome is 341 nucleotides and an internal ribosome entry site (IRES) has been proven to exist in this region [5]. Activities of IRESs of HCV were different from each genotype, and genotype IIa showed almost two-fold higher IRES activity than genotype Ib [6,7].

The IRESs have been discovered in the *Picornavirus* genomes and have a complex RNA secondary structure [5,8]. The importance of secondary structure to IRES function is understood by studies that sequence substitutions within the IRES are accompanied by compensatory mutations that act to maintain the RNA secondary structure. The 40S ribosome subunit is recruited within these IRES without binding to the m^7G cap and eIF4E [9,10]. IRESs can be classified into at least 3 groups, according to their features. IRESs derived from entero- and rhinoviruses are classified into type 1(poliovirus), and oligopyrimidine tract is located in 50–100 nucleotides past the 3′ end of the IRES [11,12]. The oligopyrimidine tract

immediately follows the 3′ end of type 2 (cardio- and aphthoviruses) IRES. Encephalomyocarditis virus (EMCV) and foot and mouse disease virus possess type 2 IRESs and utilyzes eIF4G and 4B [13,14]. The HCV and classical swine fever virus (CSFV) possess type 3 IRESs which interact directly to 40S ribosome subunit and eIF3 [15]. In addition to the requirement for eIF in each IRESs, the existence of internal initiation trans-acting factors (ITAFs) has been reported [16,17]. One of ITAFs binds to picornavirus and HCV IRES commonly is polypyrimidine tract-binding protein (PTB) [11,18–20]. PTB may work in each IRESs, however, its exact role in internal initiation has been still unclear at present. In the present study, requirement of PTB in poliovirus, EMCV and HCV IRESs has been characterized, and compared in *in vitro* translation system by depletion and complementation of PTB.

2. Materials and methods

2.1. Isolation of cDNA clones and construction of expression vectors

HCV cDNA that corresponds to nucleotide positions 1-418 (GenBank) was isolated by PCR from plasma of HCV type IIa infected patients [5], using a sense primer, 5′-GATCTAGAGCCCGCCCCCTGATGGGGGCGA-3′, and antisense primer 5′-TGTCCTGCAGTTCAAGGGCCC-3′. The amplified cDNA was digested with XbaI and AatII, and replaced with an XbaI and AatII fragment (5′UTR) of pkIV [5]. A whole cDNA which was excised by XbaI-HindIII was filled up with Klenow fragment (Takara) and cloned into StuI site of pNar3 [5], and the resulting plasmid was designated as pNII5′.

Poliovirus cDNA expression vector T7M2, CAT gene with 5′UTR of EMCV (pBSECAT) and T7CAT were constructed, as described previously [19,21].

PTB cDNA that encodes whole coding region (amino acids no. 1-531) [22] or C terminal half (amino acids no. 291-531) of PTB was synthesized by RT-PCR, and cloned into the downstream of glutathione S transferase (GST) protein in frame in pGEX-KG vector, and was designated as pGST-PTB.

2.2. Expression of PTB and production of specific antibodies

The pGST-PTB was transformed in *Esherichia coli* strain SCS-1 and induced expression with 1 mM IPTG induction. *E. coli* culture (40 ml) was peletted by centrifuge and lyzed with lysozyme (1 mg/ml) and sonicated with 1% TritonX100 and 10 mM DTT. The supernatant was reacted to Glutathione Sepharose 4B (Amersham Bioscience), cleaved by thrombin (SIGMA) and purified with ploy U Sepharose 4B (Amersham Bioscience), as described previously [22]. Rabbits or guinea pigs immunized were over four times intradermal and subcutaneously or intraperitonealy with purified recombinant whole or C-terminal half of PTB (200 μg). These hyperimmune sera were purified by the protein G Sepharose 4B (Amersham Bioscience). The anti PTB rabbit IgG was further purified by the affinity

column of PTB cross-linking Formyl Cellulofine (Seikagaku Kogyo Co.), as described by manufacturer's instruction manual.

2.3. UV cross-linking assays and immunoprecipitation

RNA probes corresponding to nucleotide(nt.) 1-341 of the HCV 5′UTR, nt. 260-833 of the EMCV 5′UTR and nt. 1-747 of the PV 5′UTR were generated by the digestion of pNII5′ with BspHI, pBSECAT with BalI and pM1(T7) with HgiAI, respectively, and transcribed by using Megascript™ T7 RNA polymerase kit (Ambion) with [α-^{32}P]UTP (NEN). Labelled RNA probes were purified by the Nuc Trap™ push columns (Stratagene). Probes ($1-5\times10^6$ cpm) were incubated with or without competitor RNA in HeLa S10 lysate (10 μg) at 30 °C for 20 min and irradiated on ice for 20 min in a UV Stratalinker (Stratagene). Unbound RNAs were digested with 10 μg of RNase A (Sigma), 200 units of RNase T1 (Gibco BRL) and 1 unit of phosphodiesterase I (Amersham Bioscience). Samples were analyzed by SDS-PAGE and dried gel was exposed to imaging plate (Fuji) or X-ray film (Kodak). Radioactivity was measured by the Bio-image analyzer BAS 2000 (Fuji).

HeLa S10 or recombinant PTB which was UV cross-linked to labeled HCV RNA was solubilyzed by single lysis buffer containing 1% NP40, reacted with affinity-purified anti-PTB Ig (4 μg) and precipitated by affigel protein A (Bio Rad) beads. Precipitated protein was further characterized by SDS-PAGE.

2.4. Immuno-depletion test

Affigel protein A (Bio Rad) 50 μl was pretreated with HeLa S10 100 μl at 37 °C for 1 h. The affinity purified anti-PTB Rabbit IgG (500 μg) was added, and rotated at room temperature for 3 h. These IgG beads were coated by 10% FCS-0.1 M phosphate buffer (pH 8.0) at 37 °C for 1 h, washed with S10 dialysis buffer (10 mM Hepes-KOH pH7.5, 90 mM KOAc, 1.5 mM $Mg(OAc)_2$), and reacted to HeLa S10 lysate (150 μl) at 4 °C overnight. The supernatants of each reaction were utilized for *in vitro* translation.

2.5. Competitive ELISA

Serocluster 'U' vinyl plate with 96 wells (Costar) was coated with affinity purified rabbit anti-PTB-C term IgG (2.5 μg/ml) at 4 °C overnight. After blocking with 1% casein PBS (−) at 25 °C for 2 h, non-treated or immunodepleted HeLa S10 lysate were added to each well, and incubate at 25 °C for 2 h. Purified recombinant PTB was used for standard and non-treated or immunodepleted HeLa S10 lysates were added to each well, and incubate at 25 °C for 2 h. Then anti-PTB guinea pig IgG (1 μg/ml) was reacted at 37 °C for 1 h, and finally anti-guineapig -IgG HRP (Dako 1:2000) was reacted at 37 °C for 1 h. *Ortho*-phenylene diamine was added to each well as substrate, and the absorbance was measured by microplate reader Model 450 (Bio Rad).

2.6. In vitro transcription and translation

Plasmids were linearized by digestion with XmnI (pNII5′), HpaI (pBSECAT) and NheI (p(M1)T7) and transcribed into RNA by Megascript™ T7 RNA polymerase kit (Ambion). RNAs were treated with DNase I, precipitated with LiCl, and quantitated by the Spectrophotometer DU64 (Beckman).

Synthetic RNAs (pNII5′ RNA; 1.0 pmol, pBSECAT; 1.8 pmol, p(M1)T7; 0.36 pmol and they were optimized for the linear phase in translation activity) were translated in HeLa S10 lysates at 37 °C for 30 min with [^{35}S]-Methionine (ICN), as described previously[5]. Translation products were analyzed using 7.5–15% gradient SDS-PAGE.

2.7. Restoration assay

Purified recombinant PTB, bovine serum albumin and ribosome salt wash (RSW) were dialyzed to S10 dialysis buffer, and added to PTB depleted or non-treated HeLa S10. RSW (total 6.7 ml) was prepared from 6.1 l of HeLa S10, as described previously [5] (kindly supplied by Dr. H. Toyoda).

3. Results

3.1. Fifty-seven and 60 kDa doublet protein bound HCV, EMCV and PV RNA

HeLa cytoplasmic proteins that were detected by UV cross-linking to ^{32}P-UTP labeled RNA derived from the HCV, EMCV, and PV 5′UTR were compared (Fig. 1). Total counts of binding proteins in HCV RNA was five times lower than those of EMCV RNA, and three times lower than those of PV-RNA (PSL; HCV 21536.9, EMCV 105622.8, PV 59307.9). Among these cytoplasmic proteins, 57 and 60 kDa doublet bands on HCV RNA,EMCV RNA and PV RNA have been identified to be PTB (Fig. 1, indicated by asterisk). According to band intensities of the 57 and 60 kDa proteins, PTB bound to EMCV IRES most abundantly, and more diminished amount of PTB bound to PV and HCV IRESs (Fig. 1).

3.2. Identification of P57/60 kDa doublet protein on HCV-RNA as PTB

HCV-IRES-binding proteins with molecular weight of 57/60 kDa were further characterized. The recombinant PTB protein was expressed in *E. coli.* in the presence of IPTG, purified by glutathione sepharose and polyU sepharose column (Fig. 2A), and reacted with affinity purified anti-PTB IgG (Fig. 2B), as described in Section 2. Labeled HCV RNA 5′UTR was cross-linked to HeLa S10 lysate, and immunoprecipitated by affinity purified anti-PTB IgG (Fig. 3). The 57 and 60 kDa doublet bands were specifically reacted to the anti-PTB IgG (Fig. 3, lane HeLa). The recombinant PTB protein was cross-linked with HCV RNA 5′UTR and precipitated with anti-PTB IgG (Fig. 3, lane PTB). These results strongly indicate that PTB

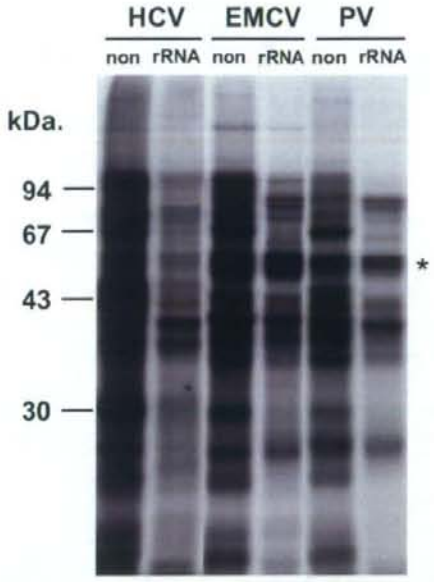

Fig. 1. UV-cross-linking analysis of binding factors to HCV, EMCV and PV-IRES RNAs. Each reaction without competitor indicates "non", and with competitor rRNA indicates rRNA on the top of the lanes. Asterisk indicates the position of PTB proteins. An asterisk indicates PTB binding.

specifically bound to HCV RNA 5′UTR, and observed as doublet protein with molecular weight of 57 and 60 kDa.

3.3. Depletion of PTB in HeLa S10 lysate

Previous results indicated the possibility that other factors than canonical eukaryotic translation initiation factors (eIFs) are working in cap independent translation. PTB is one of the candidates and when the PTB might be commonly used in several kinds of IRESs, it might play the central role in internal initiation. To compare the significance of PTB in translation initiation in HCV and other Picorna virus IRESs, PTB in HeLa S10 lysate was depleted by affinity purified anti-PTB IgG. For the depletion of PTB, pre-coating of Affi-gel protein A beads was necessary to block the non-specific adsorption, as described in Section 2. Pre-coated beads were reacted with anti-PTB IgG. From the preliminary experiments, more than 100 times higher molar ratio of anti-PTB IgG to PTB in S10 lysates was required for the over 90% depletion, as described in Materials and methods. We performed the PTB depletion, and 94.5% of PTB was depleted by anti-PTB IgG and 26.3% of PTB was depleted by pre-immune IgG (Fig. 4). We further examined the effect of PTB

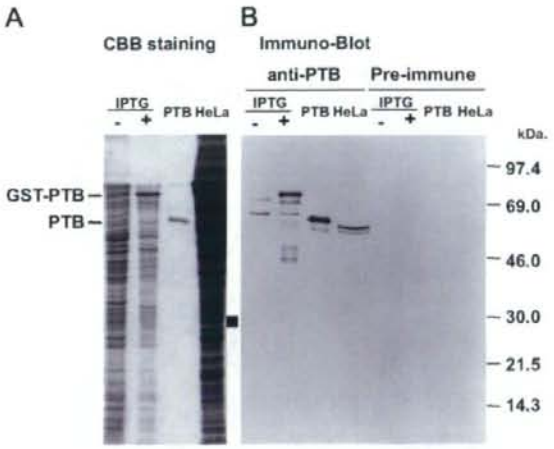

Fig. 2. Expression of recombinant PTB protein fused with GST in *E. coli*: (A) Expression of PTB protein was induced by IPTG, purified by glutathione sepharose column and stained with CBB. (B) Expressed recombinant PTB was transferred to membrane and reacted with specific antibody by WB.

depletion to the binding of cellular factors to three IRESs (Fig. 5). In PTB depleted lysates, binding of 57 and 60 kDa doublet protein was decreased, especially in PV-RNA. However, binding of other factors was not influenced significantly, other than 28 kDa protein (Fig. 5, indicated by an arrow).

3.4. *Effect of PTB depletion in translation*

Influence of PTB depletion was examined in HCV, EMCV and PV-RNA (Fig. 6A, Table 1). The reaction curves of each RNA were different from each other (data not shown), and the optimum quantity of each RNA used in this study was different from each other (Table 1). From the comparison of translation activity in PTB depleted S10 lysates, translation of PV-RNA was significantly decreased in 4 and 8 μl lysates (22–4.5%, 15–0.9%, Table 1, Fig. 6A). Translation of EMCV-IRES was significantly decreased after PTB depletion (53–44% (4 μl), 28–11% (8 μl)), but this suppression was not as much as PV-IRES. Activity of HCV-IRES was almost similar between pre-immune IgG-treated and anti-PTB IgG-treated S10 lysates. Because the optimal RNA quantities for translation are different in each IRESs, therefore, we calculated the ratio of PTB quantity per template RNA molecules (PTB/RNA) (ng/pmol; Table 1). In PV-IRES, translation activity was significantly reduced after depletion (4.5%, 0.9%) and the PTB/RNA ratio was 1.4 and 0.56. EMCV-IRES and HCV-IRES activity. Influence of PTB depletion to HCV-IRES activity was much lower than those of PV and EMCV.

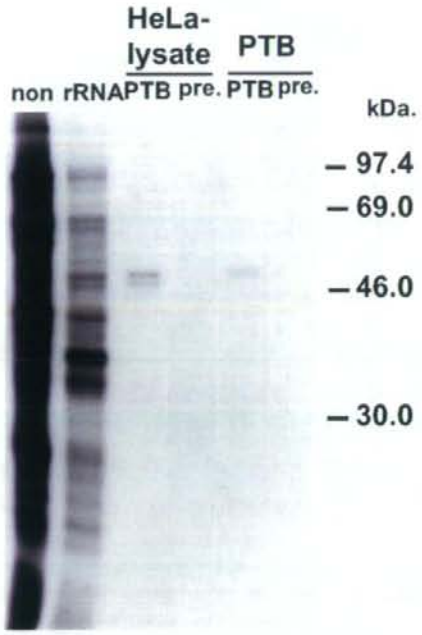

Fig. 3. HCV-IRES cross-linked S10 and PTB was immuno-precipitated by purified anti PTB antibody and pre-immune antibody. The 57 and 60 kDa doublet bands were specifically reacted to the anti-PTB IgG (lane HeLa). The recombinant PTB protein was cross-linked with HCV RNA 5′UTR and precipitated with anti-PTB IgG (lane PTB). Pre-immune antibody did not reacted to both Hela S10 and PTB.

The IRES activity of EMCV and PV-RNA was decreased by treatment of pre-immune IgG, however, treatment of pre-immune IgG did not influence significantly to the IRES activity of HCV-RNA.

3.5. Restoration of PTB to depleted S10

To clarify the effect of immuno-depletion was mainly caused by the decreased quantity of PTB, the purified recombinant PTB or RSW was added to depleted S10 (Fig. 6B). The IRES activity of PV-RNA in depleted S10 lysate (6 μl) was increased by the addition of PTB in dose-dependent manner. The EMCV-IRES activity was recovered even in the presence of 1 μg of PTB in depleted S10 lysate (4.0 μl). When too much quantity of PTB was added to the S10, translation activity of PV, EMCV and HCV decreased (over 10 times of PTB in PV, over 300 times in EMCV and over 500 times in HCV RNA, data not shown).

Translation activity of PV and EMCV-RNA became higher after the addition of RSW to anti-PTB IgG depleted S10 (150% and117%, respectively) (date not

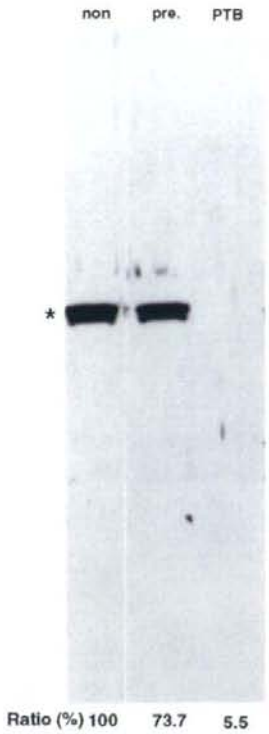

Fig. 4. Depletion of HeLa S10 by pre-immune IgG and affinity purified anti-PTB IgG. They were reacted with anti-PTB antibody by WB. Asterisk indicates the position of PTB proteins. Anti-PTB IgG deplete 94.5% of PTB (lane PTB) and pre-immune IgG deplete 26.3% of PTB (lane pre).

shown). This might indicate the existence of several translation factors other than PTB, which were lost during the treatment of IgG.

Taken together, results of this study strongly indicate that significance of PTB was highest in PV-IRES and was lowest implication in HCV-IRES.

4. Discussion

In present study, the significance of PTB in HCV, EMCV and PV IRESs has been compared. From the immuno-depletion experiment (Table 1), PTB-Ig depleted S10 (4.0 μl) contained 0.009 molecule of PTB per 1 molecule of RNA, in which PV IRES activity is 0.9%. This may indicate that almost one PTB molecule should be required

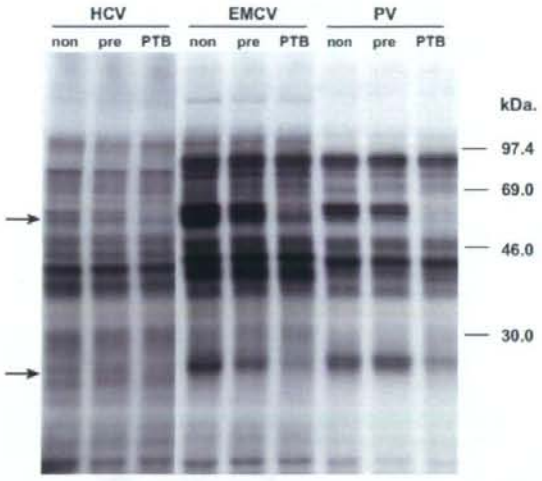

Fig. 5. UV-cross-linking analysis of HCV, EMCV and PV RNA with non-treated, pre-immune IgG-treated, and anti-PTB IgG-treated HeLa S10 lysate (lane non, pre, PTB). Upper arrow indicates the binding of PTB. Doublet protein (57 and 60 kDa) was decreased, especially in PV-RNA. Lower arrow indicates 28 kDa protein.

for 100% activity of PV IRES-RNA. In the case of EMCV IRES-RNA, 0.002 molecule of PTB per RNA gave 11% of EMCV IRES activity, and that of HCV IRES, 0.0025 molecule of PTB gave 31% of HCV IRES activity. Therefore, requirement of PTB for IRES activity was highest in PV, and less in EMCV and HCV IRES-RNA.

From the results in this study, we can compare the requirement amount of PTB in IRES activity with those of canonical eIFs. The most limiting initiation factor in cells is eIF4E, with estimates in rabbit reticulocyte lysates ranging from 0.02 copies [23] to 1 copy [24] per ribosome. The concentration of ribosomes has been estimated to be approximately 2 μM [25]. From the results of *in vitro* translation experiment, PTB should work at 0.1–0.15 M in each IRESs at maximum activity (Table 1). Therefore, working concentration of PTB for IRES activity should show almost similar to those of eIFs.

During the immuno-depletion experiment, treatment of normal IgG conjugated beads decreased the IRESs activity; 89 (6.5 μl) or 33 (3.5 μl)% in HCV IRES, 53 or 28% in EMCV IRES, and 22% or 15% in PV-IRES (Table 1). This may suggest the existence of unknown factors, which could be inactivated during the process of immuno-depletion experiment, and these effects in PV-IRES were highest among the IRESs. PV-IRES is classified into the type I [26], and the canonical eIFs with the exception of cap-binding protein eIF4E [27] and PTB [26], La [26] and 39 kDa poly(rC)-binding protein [26] are working. In EMCV IRES (type II), eIF4G was

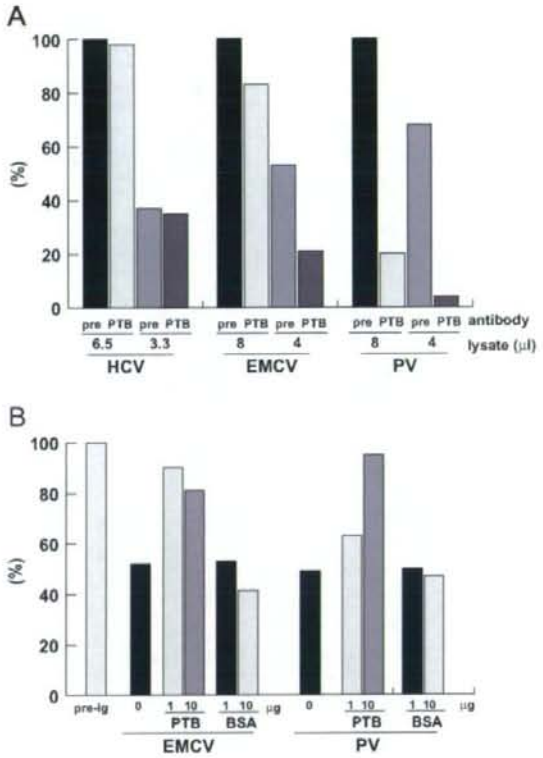

Fig. 6. (A) Effect of PTB depletion in HCV, EMCV and PV IRES. IRESs were translated in pre-immune IgG-depleted and anti-PTB IgG depleted S10 lysates (3.3, 6.5 μl in HCV-IRES, 4.0, 8.0 μl in EMCV- and PV-IRES. Translated products in SDS-PAGE were measured by image analyzer, and the quantity (PSL) of pre-immune IgG-treated S10 lysate was calculated as 100%. (B) Recovery of translation in PTB depleted S10 lysate by addition of recombinant PTB protein (1 and 10 μg. Translated products in SDS-PAGE were measured by image analyzer, and the quantity (PSL) of pre-immune IgG-treated S10 lysate was calculated as 100%.

directly bound and eIF4A and eIF4B can recruit 43S preinitiation complex which is composed of 40S ribosomal subunit and eIF3, eIF2, GTP and initiator tRNA[13]. Recent findings indicated the dependence of EMCV IRES on PTB for activity [28]. The HCV IRES possesses striking difference from type I and II IRESs, it recruits 43S preinitiation complex to initiation codon to form a 48S complex without involvement of eIF4A, 4B or 4F [29]. Thus, HCV IRES is simple and does not require most of eIFs, and might not be influenced by the depletion experiment using normal IgGs.

Table 1
Effect of PTB depletion in HCV, EMCV and PV IRES

RNA	RNA quantity (pmol)	S10 (μl)	PTB (ng)	Molar ratio of PTB to RNA	Ratio of translation (%)[a]
HCV	1.0	*Untreated*			
		6.5	7.2	0.12	100
		3.5	3.6	0.06	63
		Pre-im.-IgG			
		6.5	5.2	0.085	89
		3.5	2.6	0.045	33
		αPTB-IgG			
		6.5	0.4	0.005	87
		3.5	0.2	0.0025	31
EMCV	1.8	*Untreated*			
		8.0	8.8	0.08	100
		4.0	4.4	0.04	57
		Pre-im.-IgG			
		8.0	6.4	0.06	53
		4.0	3.2	0.03	28
		αPTB-IgG			
		8.0	0.5	0.005	44
		4.0	0.2	0.002	11
PV	0.36	*Untreated*			
		8.0	8.8	0.4	100
		4.0	4.4	0.2	65
		Pre-im.-IgG			
		8.0	6.4	0.3	22
		4.0	3.2	0.15	15
		αPTB-IgG			
		8.0	0.5	0.02	4.5
		4.0	0.2	0.009	0.9

[a]Ratio of translation products was quantitated by image analyzer.

Recent riboproteomic approach revealed the novel interacting proteins to IRESs [30], other than PTB, such as actin, forming homolog overexpressed in spleen, and microtuble interacting protein that associates with TRAF3. These factors should be characterized as novel ITAFs and comparative aspects in different IRESs should be addressed in the future work to clarify the character of each IRESs.

Acknowledgments

This work was supported by the grants from the Ministry of Health and Welfare, or Education, Culture, Sports, Science and Technology of Japan, the program for

promotion of fundamental studies in health sciences of the National Institute of Biomedical Innovation, and the Cooperative Research Project on Clinical and Epidemiological Studies of Emerging and Re-emerging Infectious Diseases.

References

[1] Choo QL, Kuo G, Weiner AJ, Overby LR, Bradley DW, Houghton M. Isolation of a cDNA clone derived from a blood-borne non-A, non-B viral hepatitis genome. Science 1989;244:359–62.
[2] Takamizawa A, Mori C, Fuke I, Manabe S, Murakami S, Fujita J, et al. Structure and organization of the hepatitis C virus genome isolated from human carriers. J Virol 1991;65:1105–13.
[3] Kato N, Hijikata M, Ootsuyama Y, Nakagawa M, Ohkoshi S, Sugimura T, et al. Molecular cloning of the human hepatitis C virus genome from Japanese patients with non-A, non-B hepatitis. Proc Natl Acad Sci USA 1990;87:9524–8.
[4] Kaito M, Watanabe S, Tsukiyama-Kohara K, Yamaguchi K, Kobayashi Y, Konishi M, et al. Hepatitis C virus particle detected by immunoelectron microscopic study. J Gen Virol 1994;75(Part 7):1755–60.
[5] Tsukiyama-Kohara K, Iizuka N, Kohara M, Nomota A. Internal ribosome entry site within hepatitis C virus RNA. J Virol 1992;66:1476–83.
[6] Kamoshita N, Tsukiyama-Kohara K, Kohara M, Nomoto A. Genetic analysis of internal ribosomal entry site on hepatitis C virus RNA: implication for involvement of the highly ordered structure and cell type-specific transacting factors. Virology 1997;233:9–18.
[7] Nomoto A, Tsukiyama-Kohara K, Kohara M. Mechanism of translation initiation on hepatitis C virus RNA. Princess Takamatsu Symp 1995;25:111–9.
[8] Pelletier J, Sonenberg N. Internal initiation of translation of eukaryotic mRNA directed by a sequence derived from poliovirus RNA. Nature 1988;334:320–5.
[9] Kieft JS, Zhou K, Jubin R, Doudna JA. Mechanism of ribosome recruitment by hepatitis C IRES RNA. RNA 2001;7:194–206.
[10] Yu Y, Ji H, Doudna JA, Leary JA. Mass spectrometric analysis of the human 40S ribosomal subunit: native and HCV IRES-bound complexes. Protein Sci 2005;14:1438–46.
[11] Hellen CU, Pestova TV, Litterst M, Wimmer E. The cellular polypeptide p57 (pyrimidine tract-binding protein) binds to multiple sites in the poliovirus 5′ nontranslated region. J Virol 1994;68:941–50.
[12] Hunt SL, Jackson RJ. Polypyrimidine-tract binding protein (PTB) is necessary, but not sufficient, for efficient internal initiation of translation of human rhinovirus-2 RNA. RNA 1999;5:344–59.
[13] Kolupaeva VG, Pestova TV, Hellen CU, Shatsky IN. Translation eukaryotic initiation factor 4G recognizes a specific structural element within the internal ribosome entry site of encephalomyocarditis virus RNA. J Biol Chem 1998;273:18599–604.
[14] Kolupaeva VG, Hellen CU, Shatsky IN. Structural analysis of the interaction of the pyrimidine tract-binding protein with the internal ribosomal entry site of encephalomyocarditis virus and foot-and-mouth disease virus RNAs. RNA 1996;2:1199–212.
[15] Sizova DV, Kolupaeva VG, Pestova TV, Shatsky IN, Hellen CU. Specific interaction of eukaryotic translation initiation factor 3 with the 5′ nontranslated regions of hepatitis C virus and classical swine fever virus RNAs. J Virol 1998;72:4775–82.
[16] Witherell GW, Wimmer E. Encephalomyocarditis virus internal ribosomal entry site RNA–protein interactions. J Virol 1994;68:3183–92.
[17] Scheper GC, Voorma HO, Thomas AA. Binding of eukaryotic initiation factor-2 and trans-acting factors to the 5′ untranslated region of encephalomyocarditis virus RNA. Biochimie 1994;76:801–9.
[18] Ali N, Siddiqui A. Interaction of polypyrimidine tract-binding protein with the 5′ noncoding region of the hepatitis C virus RNA genome and its functional requirement in internal initiation of translation. J Virol 1995;69:6367–75.
[19] Jang SK, Wimmer E. Cap-independent translation of encephalomyocarditis virus RNA: structural elements of the internal ribosomal entry site and involvement of a cellular 57-kDa RNA-binding protein. Genes Dev 1990;4:1560–72.

[20] Luz N, Beck E. Interaction of a cellular 57-kDa protein with the internal translation initiation site of foot-and-mouth disease virus. J Virol 1991;65:6486–94.
[21] Jang SK, Pestova TV, Hellen CU, Witherell GW, Wimmer E. Cap-independent translation of picornavirus RNAs: structure and function of the internal ribosomal entry site. Enzyme 1990;44:292–309.
[22] Garcia-Blanco MA, Jamison SF, Sharp PA. Identification and purification of a 62,000-Da protein that binds specifically to the polypyrimidine tract of introns. Genes Dev 1989;3:1874–86.
[23] Hiremath LS, Webb NR, Rhoads RE. Immunological detection of the messenger RNA cap-binding protein. J Biol Chem 1985;260:7843–9.
[24] Rau M, Ohlmann T, Morley SJ, Pain VM. A reevaluation of the cap-binding protein, eIF4E, as a rate-limiting factor for initiation of translation in reticulocyte lysate. J Biol Chem 1996;271:8983–90.
[25] Duncan R, Hershey JW. Identification and quantitation of levels of protein synthesis initiation factors in crude HeLa cell lysates by two-dimensional polyacrylamide gel electrophoresis. J Biol Chem 1983;258:7228–35.
[26] Flint SJ, Enquist LW, Krug RM, Racaniello VR, Skalka AM, editors. Virology. Washington, DC: ASM Press; 2000.
[27] Gingras AC, Svitkin Y, Belsham GJ, Pause A, Sonenberg N. Activation of the translational suppressor 4E-BP1 following infection with encephalomyocarditis virus and poliovirus. Proc Natl Acad Sci USA 1996;93:5578–83.
[28] Kaminski A, Jackson RJ. The polypyrimidine tract binding protein (PTB) requirement for internal initiation of translation of cardiovirus RNAs is conditional rather than absolute. RNA 1998;4:626–38.
[29] Hellen CU, Pestova TV. Translation of hepatitis C virus RNA. J Viral Hepat 1999;6:79–87.
[30] Lu H, Li W, Noble WS, Payan D, Anderson DC. Riboproteomics of the hepatitis C virus internal ribosomal entry site. J Proteome Res 2004;3:949–57.

Available online at www.sciencedirect.com
ScienceDirect
Virology 375 (2008) 321–330
VIROLOGY
www.elsevier.com/locate/yviro

Measles virus induces cell-type specific changes in gene expression

Hiroki Sato [a], Reiko Honma [b], Misako Yoneda [a], Ryuichi Miura [a], Kyoko Tsukiyama-Kohara [c], Fusako Ikeda [a], Takahiro Seki [a], Shinya Watanabe [b], Chieko Kai [a,*]

[a] *Laboratory Animal Research Center, The Institute of Medical Science, The University of Tokyo, 4-6-1 Shirokanedai, Minato-ku, Tokyo 108-8639, Japan*
[b] *Clinical Informatics, Tokyo Medical and Dental University, 1-5-45 Yushima, Bunkyo-ku, Tokyo, Japan*
[c] *Faculty of Medical and Pharmaceutical Sciences, Kumamoto University, 1-1-1 Honjo, Kumamoto City, Kumamoto, Japan*

Received 16 May 2007; returned to author for revision 13 June 2007; accepted 8 February 2008
Available online 28 March 2008

Abstract

Measles virus (MV) causes various responses including the induction of immune responses, transient immunosuppression and establishment of long-lasting immunity. To obtain a comprehensive view of the effects of MV infection on target cells, DNA microarray analyses of two different cell-types were performed. An epithelial (293SLAM; a 293 cell line stably expressing SLAM) and lymphoid (COBL-a) cell line were inoculated with purified wild-type MV. Microarray analyses revealed significant differences in the regulation of cellular gene expression between these two different cells. In 293SLAM cells, upregulation of genes involved in the antiviral response was rapidly induced; in the later stages of infection, this was followed by regulation of many genes across a broad range of functional categories. On the other hand, in COBL-a cells, only a limited set of gene expression profiles was modulated after MV infection. Since it was reported that V protein of MV inhibited the IFN signaling pathway, we performed a microarray analysis using V knockout MV to evaluate V protein's effect on cellular gene expression. The V knockout MV displayed a similar profile to that of parental MV. In particular, in COBL-a cells infected with the virus, no alteration of cellular gene expression, including IFN signaling, was observed. Furthermore, IFN signaling analyzed *in vitro* was completely suppressed by MV infection in the COBL-a cells. These results reveal that MV induces different cellular responses in a cell-type specific manner. Microarray analyses will provide us useful information about potential mechanisms of MV pathogenesis.

Keywords: Measles virus; Microarray; V protein; IFN signaling; Lymphoid cells; Epithelial cells

Introduction

During measles virus (MV) infection, the virus first enters the host via the respiratory route and replicates in tracheal and bronchial epithelial cells. The virus then enters and replicates in local lymphatic tissues and spreads through the blood to infect a variety of organs. After a latent period lasting between 10 and 14 days, patients develop symptoms, such as fever, coryza, coughing, and conjunctivitis, followed by the appearance of a characteristic rash. Immune responses have been noted to occur at almost the same time the rash fades. Recovery is accompanied by life-long immunity to reinfection. Immunosuppression, including marked lymphopenia, coincides with the appearance of immune activation and lasts for several weeks after apparent recovery (Griffin, 2001). The various pathogenic forms of measles and the different immune responses are a result of the interaction between the host and the virus. There are many *in vitro* studies on the mechanisms that trigger these reactions in MV-infected cells. For example, MV infection induces innate immune and antiviral proteins, including interferon (IFN) production in MV-infected epithelial, endothelial, and glial cells (Dhib-Jalbut and Cowan, 1993; Helin et al., 2001; Noe et al., 1999; Schneider-Schaulies et al., 1993; Vidalain et al., 2002; Yokota et al., 2004). On the other hand, some reports have demonstrated contrary results suggesting that MV does not induce the production of IFN in peripheral blood mononuclear cells (PBMC) (Naniche et al., 2000). Furthermore, recent reports have indicated that a non-structural accessory protein, the V protein, encoded within the phosphoprotein (P) gene, possesses

* Corresponding author. Fax: +81 3 5449 5379.
E-mail address: ckai@ims.u-tokyo.ac.jp (C. Kai).

0042-6822/$ - see front matter © 2008 Elsevier Inc. All rights reserved.
doi:10.1016/j.virol.2008.02.015

IFN-antagonist activity (Ohno et al., 2004; Palosaari et al., 2003; Takeuchi et al., 2003; Yokota et al., 2003). However, there are discrepancies between the various studies and the full picture remains unclear.

High-density DNA microarrays can provide a powerful approach to the profiling of the simultaneous expression of thousands of genes. Previously, Bolt et al. performed DNA microarray analysis with a limited number of human genes, approximately 3000 genes, to monitor any change in the host transcriptional profile of human PBMCs after infection with MV, and found only a few genes to be upregulated by MV infection (Bolt et al., 2002). To obtain a more comprehensive view of the overall effects of MV infection in target cells, we performed DNA microarray analysis containing more than 22,000 human genes of two different cell-types. Experiments were designed to assess gene expression patterns in human epithelial and lymphoid cells, which are the cell-types that are targeted during the pathogenesis of primary MV infection. A significant difference between these cells was observed. More recently, Zilliox et al. reported a microarray analysis of MV-infected dendritic cells and identified numerous genes that were regulated by MV (622 upregulated and 931 downregulated genes) (Zilliox et al., 2006). The profile of altered gene expression in dendritic cells was similar to that in epithelial cells in our results. Interestingly, cell-type specific modulation of the IFN signaling pathway was identified in the present study. In addition, to evaluate the effect of V protein on the modulation of host gene expression, we generated V knockout MV by employing a reverse genetics system and performed microarray analysis. The present study provides an additional comprehensive view of MV effects on different cells.

Results

Preparation of cells and virus

Experiments were designed to assess patterns of gene expression in human epithelial and lymphoid cells, which are the cell-types that are targeted during the pathogenesis of primary MV infection. First, we established a human epithelial cell line that was sensitive to wild-type MV infection. We took 293 human embryonic kidney epithelial-like cells and transfected them with the signaling lymphocytic activation molecule (SLAM) gene, a receptor for wild-type MV (Tatsuo et al., 2001). The cells were highly susceptible to MV infection and showed a large syncytium post infection (data not shown). These cells were designated 293SLAM cells. To compare transcriptional response between different cell-types after MV infection, we used a novel established human lymphoid cell line, COBL-a, which was established from a cultured umbilical cord blood cell colony (Kobune et al., 2007). COBL-a cells are a T cell lineage cell line expressing CD4 (helper-T), CD38 (immature T), CD46, and CD150 (SLAM). Cells are highly sensitive to MV infection and cause CPE post infection. In addition, a wild-type MV isolated from a blood specimen using the COBL-a cells maintained pathogenicity specific for typical acute measles against cynomolgus monkeys. The COBL-a cells are therefore ideal for virus propagation and subsequent microarray assays.

We used the HL strain (Kobune et al., 1996) as a wild-type MV. MV-HL was isolated from blood leukocytes of a patient with typical measles and induced the typical clinical signs of measles, including rashes, Koplik's spots, and transient marked leukopenia in cynomolgus and squirrel monkeys. Thus, MV-HL is considered to possess the pathogenicity of acute measles. The HL strain grew well, both in COBL-a cells and 293SLAM cells, reaching a similar maximum titer in both cells (Fig. 1). Since MV-HL is propagated on B95a cells, a marmoset B-cell line transformed with Epstein–Barr virus (EBV) (Kobune et al., 1990), it was passaged twice in 293SLAM cells that were insensitive to EBV to eliminate EBV in the MV stock solution. The obtained virus solution was inoculated onto COBL-a cells and, after 3 days, no EBV contamination was confirmed by RT-PCR using EBV specific primer pairs (Teng et al., 1996) (data not shown). To obtain the necessary quantity of MV, it was propagated largely in COBL-a cells and was then purified by ultracentrifugation.

Overview of expression microarray analysis

COBL-a cells and 293SLAM cells were inoculated with purified MV at a multiplicity of infection (MOI) of 2 to ensure that every cell was in contact with infectious viral particles. Mock and infected cells were harvested at 6, 12, and 24 h post infection and isolated poly(A+) RNAs were labeled with Cyanine 3-dUTP or Cyanine 5-dUTP. The labeled samples were hybridized on microarrays representing 22,272 human genes. Hybridization signals were processed into expression ratios as log 2 values (designated mean log ratios; see Materials and methods). The genes with mean log ratios over 1 or under −1 in at least one sample were extracted, and cluster analysis was carried out. Data from all the arrays used in this paper are available at DDBJ via CIBEX (http://www.cibex.nig.ac.jp/cibex/HTML/index.html) under accession number CBX32. Interestingly, significant differences in the regulation of cellular gene expression were observed between 293SLAM and COBL-a cells (Fig. 2). The number of genes that were up- and downregulated with a mean log ratio over 1 or under −1 in individual samples is shown in Fig. 2B. In 293SLAM cells,

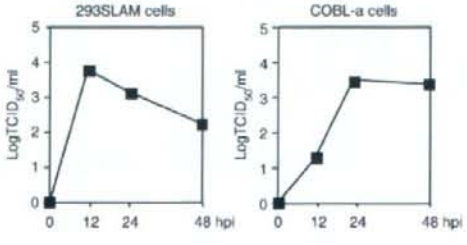

Fig. 1. Comparison of the replication of MV-HL in 293SLAM and COBL-a cells. After infection at an MOI of 0.001, the viral titer was determined by $TCID_{50}$ at the indicated time points. The average of two independent measurements is shown.

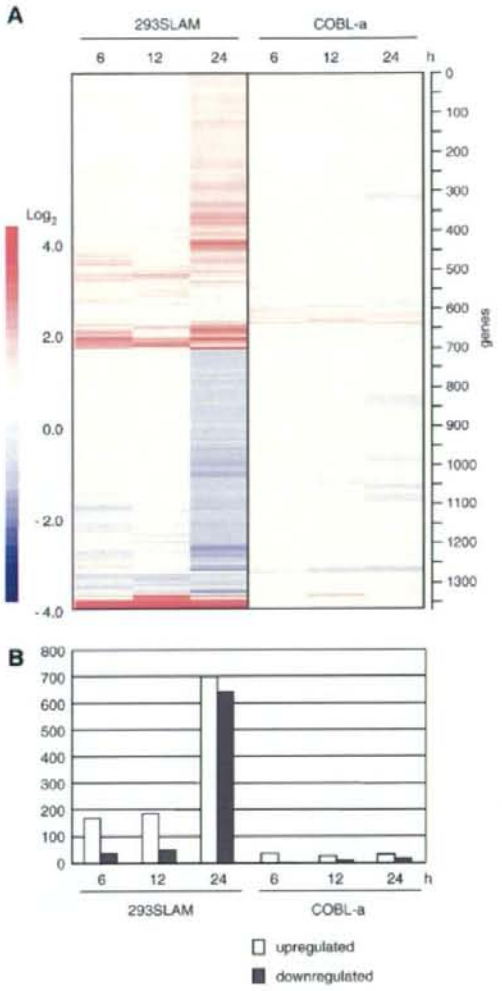

Fig. 2. Gene expression profiles of 293SLAM cells and COBL-a cells inoculated with MV-HL. (A) Genes exhibiting the mean log ratio in all 6 samples were extracted (19,415 genes). These genes were further extracted with |mean log ratio| ≥ 1, and the resulting 1,368 genes were assembled in the order obtained from the results of hierarchical clustering analysis. The y-axis of the dendrogram depicts Euclid square distance as the dissimilarity coefficient. The color bar on the left side of the figure shows expression ratio against mock-infected RNA in $\log_2$; red and blue indicate increase and decrease of mean log ratios, respectively. (B) Kinetics of changes in total gene expression after MV infection. Individual values for genes upregulated and genes downregulated by MV infection were represented graphically.

marked cellular responses were induced by MV infection, and the number of regulated genes increased over time. On the other hand, COBL-a cells showed little alteration in gene expression despite similar viral replication rates as those observed in 293SLAM cells.

Effects of MV on gene expression in 293SLAM cells

In 293SLAM cells, a series of cellular genes was found to be upregulated and downregulated by virus infection. Among genes that were altered early (6 h post infection), the most apparent characteristic was the upregulation of a series of genes that are related to innate immune and antiviral responses. This result clearly showed typical early events after virus infection, such as activation of IRF-3 and NF-kB, which result in the induction of type I IFN. Furthermore, a series of IFN signal transductions was subsequently observed. In particular, the three principal families of IFN-inducible genes (RNA-activated protein kinase [PKR], the 2′5′-oligoadenylate synthetases [OAS], and the Mx proteins) were markedly induced. In addition, activation of a broad range of functional responses that are involved in the host antiviral response, including many IFN-stimulated genes (ISG), inflammatory cytokines, and immune pathways, was demonstrated. These results show that MV infection and replication trigger a rapid and strong innate antiviral response in 293SLAM cells. The number of upregulated genes was slightly increased 12 h post infection (Fig. 2B).

At 24 h post infection, the number of upregulated genes increased significantly; 701 upregulated genes were identified. To facilitate the analysis of our data, we grouped the regulated genes according to biological functions (Table 1). Upregulation

Table 1
Classes of genes upregulated at 24 h post MV infection in 293SLAM cells

Functional classification	Number
Antivirus	60
Metabolism	31
Transcription factor, transcription regulation	30
Zinc finger protein	24
Protein kinases and phosphatases	21
Channels and transporters	18
Nucleus and nuclear matrix	16
Histocompatibility and cell surface markers	15
Oncogenesis	13
Cytoskeleton and cell structure, motor protein	13
Protein degradation	9
Apoptosis, antiapoptosis	9
Cellular development and differentiation, physiology	8
Growth factor	8
RNA processing and binding modification	8
Cell adhesion and intercellular junction, extracellular matrix	7
Cell cycle related	7
Stress response/cell defense	6
Receptor and receptor-associated	6
tRNA	6
DNA modification and replication	5
Vesicular protein trafficking and fusion, vesicular formation	5
Immunity	4
Intracellular transporter	4
Signaling	3
Hormone related	3
Homeostasis	3
Protein modification	1
Translation	1
Unknown function	49
Hypothetical protein	308
Total	701

Table 2
Classes of genes downregulated at 24 h post MV infection in 293SLAM cells

Functional class	Number
Metabolism	108
Protein degradation	35
Cytoskeleton and cell structure, motor protein	27
Ribosomal proteins	26
Protein modification	21
Cellular development and differentiation, physiology	20
Cell adhesion and intercellular junction, extracellular matrix	19
Nucleus and nuclear matrix	19
Transcription factor, transcription regulation	16
Receptor and receptor-associated	14
Protein kinases and phosphatases	11
Channels and transporters	11
Signaling	11
Stress response/cell defense	11
RNA processing and binding, modification	11
Immunity	8
Histocompatibility and cell surface markers	7
Cell cycle related	7
Vesicular protein trafficking and fusion, vesicular formation	7
Intracellular transporter	7
Homeostasis	7
Antivirus	5
Oncogenesis	5
Apoptosis, antiapoptosis	5
Zinc finger protein	3
Growth factor	3
Translation	3
Hormone related	1
DNA modification and replication	1
Unknown function	60
Hypothetical protein	152
Total	641

of a series of antiviral genes observed at 6 h post infection persisted until 24 h post infection. Many genes that are implicated in broad biological functions were upregulated, in particular, cellular signal transducers, such as transcription factors, zinc finger proteins, protein kinases, and phosphatases, were induced. This result suggests that, during the late stages of MV infection, MV replication strongly induces the expression of many genes that control multiple cellular functions. About half of the upregulated genes were classified as hypothetical or unidentified genes.

The number of downregulated gene in 293SLAM cells was also greatly increased 24 h post infection (Fig. 2B). A total of 641 genes were identified. Many of the downregulated genes could be classified in restricted categories (Table 2). The majority of genes that were downregulated were so-called 'housekeeping genes'. In particular, a large quantity of mitochondrial protein genes, including those involved in the electron transport system and energy metabolism, were downregulated. Furthermore, most ribosomal proteins, including mitochondrial ribosomal proteins, were downregulated. In addition, many genes implicated in the cytoskeleton, cell structure and enzymes of the glycolytic pathway and lipid metabolism were also downregulated. These observations suggest that, during later stages of infection, MV infection induced deficient maintenance of overall cellular function.

MV infection induced a biphasic modulation of gene expression in 293SLAM cells; in the early stage, a series of antiviral gene expressions were rapidly induced, and during the later stages of infection, MV replication modulated the expression of genes across a broad range of functional categories.

Effects of MV on gene expression in COBL-a cells

In COBL-a cells, only limited sets of gene expression profiles were modulated after MV infection. In fact, 24 h post infection, only 23 genes were upregulated (Table 3). In contrast to that seen in 293SLAM cells, the series of genes involved in innate antiviral responses was not altered, other than a single cytokine. This result in COBL-a cells suggests that MV suppresses expression of genes involved in the host antivirus system and the IFN-α/β signaling pathway. Only 17 genes were downregulated in COBL-a cells 24 h post infection (Table 4). Many of these genes were related to metabolic enzymes involved in sterol and fatty acid. All of these genes were also downregulated in 293SLAM cells. This suggests that the downregulation signal of MV infection was partially and weakly conserved between 293SLAM and COBL-a cells.

Effect of recombinant MV lacking V protein on gene expression

As with other paramyxoviruses, MV produces two non-structural accessory molecules, the C and V proteins, encoded within the phosphoprotein gene. In MV, several reports have

Table 3
Upregulated at 24 h post MV infection in COBL-a cells

Gene name	cDNA accession no.	Fold increase (log2)
Dehydrogenase/reductase (SDR family) member 2 (DHRS2), mRNA	NM_005794	2.2301
Rhabdoid tumor deletion region gene 1 (RTDR1), mRNA	NM_014433	1.8515
PRO1768 protein (PRO1768), mRNA	NM_014099	1.6207
Ras protein-specific guanine nucleotide-releasing factor 1 (RASGRF1)	NM_002891	1.5769
KIAA0590 gene product (KIAA0590), mRNA	NM_014714	1.4823
cDNA FLJ30514 fis, clone BRAWH2000682	AK055076	1.4243
Titin (TTN), transcript variant novex-3	NM_133379	1.404
Crystallin, beta A1 (CRYBA1), mRNA	NM_005208	1.3464
cDNA FLJ37863 fis, clone BRSSN2015907	AK095182	1.2957
cDNA FLJ30520 fis, clone BRAWH2000866	AK055082	1.2934
LOC135666 (LOC135666), mRNA	XM_069484	1.2514
cDNA FLJ fis, clone PLACE6000414	AK122657	1.1769
cDNA FLJ31592 fis, clone NT2RI2002447	AK056154	1.141
cDNA FLJ35408 fis, clone SKNSH2008969	AK092727	1.139
Hypothetical gene supported by AF007152	XM_032158	1.1382
cDNA FLJ13701 fis, clone PLACE2000223	AK023763	1.1294
cDNA FLJ10500 fis, clone NT2RP2000369	AK001362	1.1278
Similar to IGE-BINDING PROTEIN (LOC120889), mRNA	XM_062339	1.1235
cDNA FLJ35884 fis, clone TESTI2008960	AK093203	1.0978
Similar to cellular retinaldehyde-bindin	XM_069035	1.081
cDNA FLJ fis, clone BRACE2032329	AK124476	1.0558
Transient receptor potential cation channel, subfamily V, member 4 (TRPV4)	NM_021625	1.0507
Small inducible cytokine A4 (SCY A4), mRNA	NM_002984	1.0031

shown that the V protein possesses IFN-antagonist activity. To evaluate the involvement of V protein in host gene expression during MV infection, we established a reverse genetics system for MV-HL (Yoneda et al., unpublished data). Using the infectious clone, we succeeded in generating recombinant MV lacking V protein expression. We performed a microarray analysis using the V knockout MV. As shown in Fig. 3A, V knockout MV-infected cells had a similar expression profile to that of parental MV. In 293SLAM cells, rapid induction of innate immune and antiviral responses was observed, similar to that seen during parental MV infection. At 24 h post infection, V knockout MV displayed slightly weak modulation of host gene expression, but the categories of regulated genes highly overlapped with that of parental MV. Interestingly, in COBL-a cells, no alteration of cellular gene expression, including IFN signaling, was observed with V knockout MV.

To confirm the early steps of IFN signaling during MV-HL and V knockout MV infection, we examined tyrosine phosphorylation of signal transducer and activator 1 (STAT1) which is induced by IFN response. COBL-a cells and 293SLAM cells were infected with MV-HL or V knockout MV, and the cell lysates were subjected to western blotting. As shown in Fig. 3B, similar levels of tyrosine-phosphorylated STAT1 (pY-STAT1) were detected in 293SLAM cells infected with both MV-HL and V knockout MV. On the other hand, pY-STAT1 was not detectably induced in COBL-a cells after MV-HL and V knockout MV infection. Protein levels of STAT1 did not show significant differences between uninfected and infected cells of COBL-a and 293SLAM.

Table 4
Downregulated genes at 24 h post MV infection in COBL-a cells

Gene name	cDNA accession no.	Fold increase (log2)
Stearoyl-CoA desaturase (delta-9-desaturase) (SCD)	NM_005063	−1.4765
Sterol-C4-methyl oxidase-like (SC4MOL)	NM_006745	−1.3768
Fatty acid desaturase 2 (FADS2)	NM_004265	−1.3506
Epidermal growth factor receptor pathway substrate 8 (EPS8)	NM_004447	−1.2887
Midline 1 (Opitz/BBB syndrome) (MID1), transcript variant 1	NM_000381	−1.1804
Isopentenyl-diphosphate delta isomerase (IDI1)	NM_004508	−1.1777
7-dehydrocholesterol reductase (DHCR7)	NM_001360	−1.165
Hypothetical protein FLJ11700 (FLJ11700)	NM_024892	−1.1487
Insulin induced gene 1 (INSIG1)	NM_005542	−1.1149
Acetyl-coenzyme A acetyltransferase 2 (acetoacetyl coenzyme A thiolase)	NM_005891	−1.113
Lipase A, lysosomal acid, cholesterol esterase (Wolman disease) (LIPA)	NM_000235	−1.083
24-dehydrocholesterol reductase (DHCR24)	NM_014762	−1.0687
Cytochrome P450, 51 (lanosterol 14-alpha-demethylase) (CYP51)	NM_000786	−1.0677
LIM and cysteine-rich domains 1 (LMCD1)	NM_014583	−1.047
Sialyltransferase 1 (beta-galactoside alpha-2, 6-sialytransferase) (SIAT1)	NM_003032	−1.0333
cDNA FLJ36451 fis, clone THYMU2013757	AK093770	−1.0286
3-hydroxy-3-methylglutaryl-coenzyme A synthase 1 (soluble)	NM_002130	−1.0104

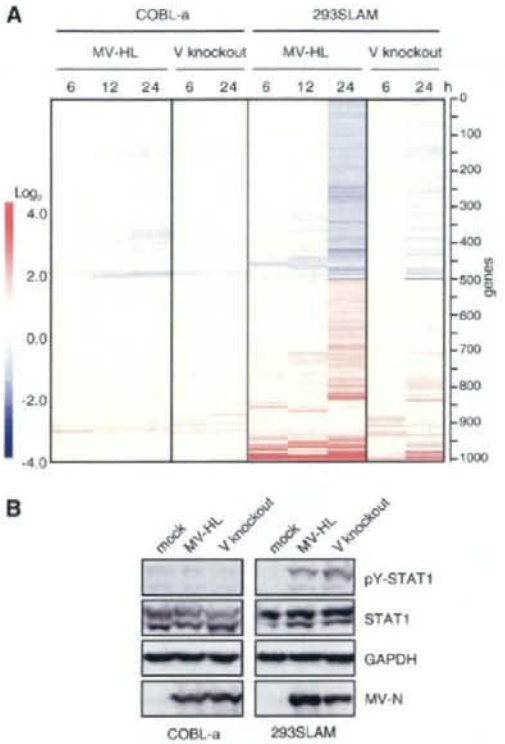

Fig. 3. Effect of recombinant MV lacking V protein on gene expression. (A) Comparison of the expression profiles between parental MV and V knockout MV. 293SLAM and COBL-a cells were inoculated with MV-HL or V knockout MV. Genes exhibiting the mean log ratio in all 10 samples were extracted (11,829 genes). These genes were further extracted with |mean log ratio| ≥ 1, and the resulting 1,012 genes were assembled in the order obtained from the results of hierarchical clustering analysis. The y-axis of the dendrogram depicts Euclid square distance as the dissimilarity coefficient. The color bar on the left side of the figure shows the expression ratio against mock-infected RNA in $\log_2$; red and blue indicate increase and decrease of mean log ratios, respectively. (B) STAT1 activating tyrosine phosphorylation was tested by western blotting with STAT1 phosphopeptide-specific antibody in COBL-a cells and 293SLAM cells infected with mock, MV-HL or V knockout MV. Total STAT1 level, GAPDH and MV-N protein expression were analyzed in parallel.

Given these data, there is little difference in host gene expression between MV-HL and V knockout MV, and V protein is considered to have little effect on changing cellular gene expression, in particular the series of genes responsible for IFN, during virus replication.

MV suppresses the IFN signaling pathway in COBL-a cells but not in 293SLAM cells

As assessed by microarray analysis, the modulation of host gene expression profile induced by MV infection was different in epithelial versus lymphoid cells. In particular, in the early period of infection, it appeared that the antiviral responses, including the expression of genes responsible for IFN, were not

induced in COBL-a cells. To confirm whether the IFN signaling pathway functions normally in COBL-a cells, we analyzed changes in gene expression that occurred in response to IFN treatment. 293SLAM cells and COBL-a cells were treated with IFN-α for 24 h, and microarray analysis was performed. The number of upregulated genes with a mean log ratio greater than 1 included 65 genes in COBL-a cells and 49 genes in 293SLAM cells; the gene expression profiles, including the upregulation of IFN-stimulated genes, was similar in these two cell lines. This result indicates that the essential IFN signaling pathway in COBL-a cells was functioning normally. Taken together with profiles after MV infection, it appears that MV infection suppressed this pathway in COBL-a cells but not 293SLAM cells. Therefore, we examined the effects of V protein expression and MV infection on IFN signaling in these two cell-types using a luciferase reporter gene which was under the control of the interferon signaling response element (ISRE). Treatment with IFN-α increased luciferase activity by about 5.6- and 4.0-fold in mock-infected 293SLAM and COBL-a cells, respectively, compared to untreated controls (Fig. 4). In both 293SLAM and COBL-a cells plasmid-expressed V protein completely abolished IFN-α induced activation of the ISRE (Fig. 4). On the other hand, in MV-infected 293SLAM cells, IFN-α-induced reporter activity was further increased and reached a 10.9-fold increase compared to untreated controls (Fig. 4), suggesting that MV-induced synergistic ISRE activation. In contrast, MV infection induced very little IFN signaling in COBL-a cells (Fig. 4), which was consistent with microarray analysis results. Interestingly, additional treatment with IFN-α did not induce synergistic activation but rather suppressed the activity of the IFN signaling pathway; there was only a 1.6-fold increase in activity in COBL-a cells compared to untreated controls (Fig. 4). These results indicate that MV infection in COBL-a cells strongly suppresses the activity of the IFN signaling pathway.

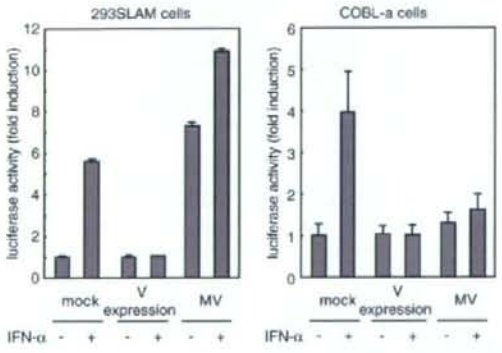

Fig. 4. MV infection inhibits IFN-α/β signaling in COBL-a but not 293SLAM cells. (A) 293SLAM cells and (B) COBL-a cells were cotransfected with an ISRE-luciferase (firefly) reporter gene, a control renilla luciferase gene, with or without V-expression plasmid. After 42 h, cells were infected with mock or MV-HL at an MOI of 2 for 6 h, and then treated with 1000 U of IFN-α per ml for 24 h. Relative expression levels were normalized by renilla luciferase activity, and the activation increase is reported as fold activation.

Discussion

We analyzed the expression of approximately 22,000 human genes during MV infection in an epithelial (293SLAM cells) and lymphoid (COBL-a cells) cell line using DNA microarrays, and identified different profiles.

In 293SLAM cells, MV infection induced rapid and strong host innate immune and antiviral responses. Host innate immune responses are the first line of defense against infections. Previously, various groups have reported that MV infection induces innate immune responses, such as: activation of NF-κB and IRF-3 transcription factors (Helin et al., 2001; Servant et al., 2001); IFN biosynthesis (Helin et al., 2001; Naniche et al., 2000); production of several cytokines (interleukin[IL]-6,-8, RANTES) (Helin et al., 2001; Sato et al., 2005); activation of IFN-stimulated gene factor 3 and GAF signaling complexes (Helin et al., 2001); induction of IRF-1 and -7 (tenOever et al., 2002; Yokota et al., 2004); and induction of immediate-early genes and genes linked to antiviral responses (Bolt et al., 2002; Helin et al., 2002). In addition to *in vitro* experiments, we have also studied the pathogenicity of MV-HL in cynomolgus monkeys, and found that type I IFN and several cytokines were transiently detected in the serum after inoculation (Sato et al., 2008). In the present study, microarray analysis clearly showed that MV infection induced innate immune and antiviral responses in 293SLAM cells, indicating that our microarray analysis was generally in agreement with previous reports. Recently, Zillox et al. reported that MV-infected dendritic cells also induced activation of antiviral responses and downregulation of housekeeping genes (Zilliox et al., 2006), coincident with our present study. A notable difference was that no induction of PKR was observed in dendritic cells (Zilliox et al., 2006) whereas, in our study, 293SLAM cells displayed clear upregulation of PKR after MV infection. This difference may be due to the cell-type.

In addition to antiviral responses, the later stage of infection showed comprehensive upregulation and downregulation of host gene expression in 293SLAM cells (Fig. 2). Previous microarray analysis reports stated that during various virus infection and replication, the genes induced by antiviral responses, such as those that are involved in the activation of NF-κB (O'Donnell et al., 2006; Tian et al., 2002) and IRF-3 (Fredericksen et al., 2004; Grandvaux et al., 2002a), were only part of the overall virus-induced gene expression profile that occurred. In addition, our data indicate that type I IFN-induced upregulation of only 49 genes in 293SLAM cells. Thus, it is likely that most of the modulated gene expression that occurs during the later stage of MV infection in 293SLAM cells is due to cellular responses to MV as a result of the accumulation of viral replication products and/or an increase in CPEs. Indeed, we used UV-inactivated MV and showed that there was no alteration of gene expression in 293SLAM cells 6 h and 24 h post inoculation (data not shown). Therefore, alteration in gene expression could not be triggered simply through signaling at the cell surface, but requires virus replication and/or accumulation of viral components in the cell. The activating signals that control expression of MV-inducible genes require further investigation.

While MV grew comparably in COBL-a and 293SLAM cells (Fig. 1), gene expression, including the expression of IFN-inducible genes, was affected very little by MV infection in COBL-a cells (Fig. 2). This result is in agreement with a previous study showing that wild-type MV had the capacity to suppress the induction of IFN-α/β in PBMCs (Naniche et al., 2000). In contrast to our microarray analysis of COBL-a cell, Bolt et al. reported that wt-MV-infected PBMCs upregulated IFN-β and IRF-7 (Bolt et al., 2002). The MV solution Bolt used contained EBV because the MV was propagated in an EBV-transformed cells. EBV probably affected the gene expression, because cytomegalovirus in the same family as EBV upregulates many cytokine gene expressions (Zhu et al., 1998). Indeed, we performed a preliminary microarray experiment using B95a-passaged MV-HL and found that several factors, including IFN-β and IRF-7, were upregulated (data not shown).

After MV infection, COBL-a cells induced low but apparent IFN levels (data not shown); however, the series of genes involved in innate antiviral responses was not upregulated (Table 3). Usually, low levels of IFN production can induce amplification of IFN production by a cellular autocrine mechanism via IFN signal transduction (Grandvaux et al., 2002b). However, in MV-infected COBL-a cells, amplification of IFN secretion was not observed. In addition, the IFN reporter assay showed that IFN-α treatment induced IFN signal transduction effectively although MV infection strongly suppressed transduction in COBL-a cells (Fig. 4). These results indicate that, in COBL-a cells, the essential IFN production capability and the IFN signaling pathway function normally, but MV infection abrogates IFN signal transduction.

It has previously been reported that the V protein of MV is involved in the inhibition of IFN signaling processes by inhibition of IFN-induced STAT nuclear translocation (Palosaari et al., 2003), the inhibition of STAT1 and STAT2 phosphorylation (Takeuchi et al., 2003), and the suppression of Jak phosphorylation (Yokota et al., 2003). We also confirmed that the V protein of MV-HL, expressed by a mammalian expression plasmid, completely suppresses IFN signaling in both 293SLAM and COBL-a cells (Fig. 4). However, as shown in Fig. 3A, in COBL-a cells, V knockout MV caused little change in cellular gene expression, including IFN signaling. The V knockout MV grew as well as the parental MV-HL (data not shown). Given these data, during virus replication, V protein appeared to have little effect on alteration of cellular gene expression, in particular the series of IFN responsible genes. Thus, in COBL-a cells, other factor(s) might also act as IFN-antagonist. In contrast, in MV-infected 293SLAM cells, IFN signaling was not blocked by MV infection (Fig. 4). Thus, V protein does not act as an IFN-antagonist or inadequately suppresses the IFN signaling pathway in MV-infected 293SLAM cells. These results indicate that plasmid-expressed V protein can interfere with IFN signal transduction in various cells including 293SLAM cells, but that during MV infection, other factors may counteract and/or overcome the inhibitory effect of V protein, depending on the specific cell-type. The mechanism of cell-type specific inhibition will need to be identified in order to clarify the function of the viral proteins during MV replication.

In addition to host antivirus responses, a number of changes in gene expression observed in 293SLAM cells 24 h post infection were not detected in COBL-a cells. Interestingly, *in vitro* MV-induced immunosuppression is cell-type dependent. The proliferation rates of lymphoid cells, such as peripheral blood leucocytes, human T-cells, B cells, and monocytic cell lines, were significantly reduced by MV infection. On the other hand, no such effects were observed in cells of nonlymphoid origin (Schlender et al., 1996). In addition, a recent study found that IFN-γ-mediated antivirus activity against MV is caused in epithelial, endothelial, and astroglial cells, but not in lymphoid and neuronal cell lines (Obojes et al., 2005). These data imply that cellular factors specific for lymphoid cells are implicated in specific responses observed during MV infection and replication. In the present paper, we focused on the analysis of IFN signal transduction suppression. In future, modification of other pathways should be analyzed in detail.

This microarray analysis will help uncover new clues for analyzing the behaviour of host genes in response to infection, and the role of viral proteins in the context of MV infection.

Materials and methods

Cell culture

B95a cells and COBL-a cells were grown in RPMI1640 medium with 100 U penicillin per ml, 100 μg streptomycin per ml, and 5% (B95a cells) or 10% (COBL-a cells) fetal calf serum (FCS), at 37 °C in a 5% CO_2 incubator. Human embryonic kidney 293 cells and their derivatives were grown in Dulbecco minimal essential medium with 10% FCS, penicillin, and streptomycin at 37 °C in a 5% CO_2 incubator.

Establishment of 293SLAM cells

In order to establish epithelial cell lines stably expressing SLAM, total RNA was isolated from B95a cells using ISOGEN (NipponGene) and reverse transcribed with SuperScript II reverse transcriptase (Invitrogen) and random primer (9-mer), according to the manufacturer's instructions. The cDNA of SLAM was amplified with a specific primer pair flanking the *Eco*RI site, and then introduced into the pCAGGS mammalian expression vector (pCAG-SLAM) (Tokui et al., 1997). One μg of pCAG-SLAM and 0.1 μg of pcDNA3.1 encoding the neomycin resistance gene (Invitrogen) were cotransfected with FuGENE6 transfection reagent (Roche) into 293 cells seeded on a 10-cm dish, according to the manufacturer's instructions. Cells were then cultured in the presence of 100 μg/ml of G418. A clone expressing the highest level of SLAM (293SLAM cells) was selected for use in the following experiments.

Virus growth

293SLAM cells and COBL-a cells (1×10^6 per six-well plate) were infected with MV-HL at an MOI of 0.001 for 1 h. The inoculum was removed, and the cells were washed once with medium and then incubated in medium containing 5% FCS.